

# Spatial patterns in ant colonies

Guy Theraulaz<sup>\*†</sup>, Eric Bonabeau<sup>\*§</sup>, Stamatios C. Nicolis<sup>¶</sup>, Ricard V. Solé<sup>‡||</sup>, Vincent Fourcassié<sup>\*</sup>, Stéphane Blanco<sup>\*\*</sup>, Richard Fournier<sup>\*\*</sup>, Jean-Louis Joly<sup>\*\*</sup>, Pau Fernández<sup>||</sup>, Anne Grimal<sup>\*</sup>, Patrice Dalle<sup>††</sup>, and Jean-Louis Deneubourg<sup>¶</sup>

<sup>\*</sup>Laboratoire d'Ethologie et Cognition Animale, Centre National de la Recherche Scientifique, Formation de Recherche en Evolution 2382, <sup>††</sup>Equipe Traitement et Compréhension d'Images, IRIT, and <sup>\*\*</sup>Laboratoire d'Energétique, Université Paul Sabatier, 118 Route de Narbonne, 31062 Toulouse Cédex 4, France; <sup>‡</sup>Santa Fe Institute, 1399 Hyde Park Road, Santa Fe, NM 87501; <sup>§</sup>Eurobios, 9 Rue de Grenelle, 75007 Paris, France; <sup>¶</sup>Center for Nonlinear Phenomena and Complex Systems, CP 231, Université Libre de Bruxelles, Boulevard du Triomphe, 1050 Brussels, Belgium; and <sup>||</sup>Complex Systems Group, Departament de Física i Enginyeria Nuclear, Universitat Politècnica de Catalunya, Sor Eulàlia d'Anzizu s/n, Campus Nord, Mòdul B4, 08034 Barcelona, Spain

Communicated by I. Prigogine, Free University of Brussels, Brussels, Belgium, May 20, 2002 (received for review January 8, 2002)

**The origins of large-scale spatial patterns in biology have been an important source of theoretical speculation since the pioneering work by Turing (1952) on the chemical basis of morphogenesis. Knowing how these patterns emerge and their functional role is important to our understanding of the evolution of biocomplexity and the role played by self organization. However, so far, conclusive evidence for local activation–long-range inhibition mechanisms in real biological systems has been elusive. Here a well-defined experimental and theoretical analysis of the pattern formation dynamics exhibited by clustering behavior in ant colonies is presented. These experiments and a simple mathematical model show that these colonies do indeed use this type of mechanism. All microscopic variables have been measured and provide the first evidence, to our knowledge, for this type of self-organized behavior in complex biological systems, supporting early conjectures about its role in the organization of insect societies.**

Many biological systems display large-scale features involving some characteristic scale that is much larger than the size of its individual components (1). These structures are observed in a broad range of systems and scales, from animal coats (2), shell patterns (3, 4), and neural structures (5) to the spatial distribution of individuals in ecosystems (6). In many cases, they reflect functionality and adaptation and in all of them, they provide clues for the underlying rules that generate them. In most cases, it is clear that the information available to individual units is gathered from a local neighborhood much smaller than the resulting structures, suggesting some type of amplification mechanism that relies on collective behavior.

The first theoretical explanation of these types of structures was suggested in 1952 by Alan Turing (1, 7, 8). The basic mechanism at work involves local amplification of fluctuations (activation) and long-range inhibition and actually falls within a general class of mechanisms (9–12). These mechanisms have been identified in physical (13) and chemical (14) systems, in ecosystems (2, 6, 10, 15–18) and morphogenesis (2–5, 11, 19–26). In the slime mold (27, 28), the evidence is also strong. Critics have argued that a proof requires the identification and measurement of the microscopic mechanisms at work, and this is obviously a rather difficult task in biology.

In this context, it was early suggested that social insects might actually use these types of mechanisms to build their nests (29, 30) and produce a wide variety of spatiotemporal structures (31–34). Here we use social insects and their behavioral patterns of organization as our reference system. We follow a standard approach, using a well-defined and controlled experimental setup in which the whole set of parameters can be measured and therefore all of the microscopic rules can be identified. We show that the formation of cemeteries in ants (35–38) falls within the family of local activation–long range inhibition (LALI) processes originally suggested by Gierer and Meinhardt (9), the inhibition resulting from the depletion of the substrate. In experiments carried out with the ant *Messor sancta*, we confirm the presence

of self-organization dynamics as responsible for the regular structures generated by the clustering process, and a mathematical model is presented, consistently reproducing the experimental observations.

## Methods

**Colony Collection and Ant Maintenance.** Experiments were carried out with colonies of the ant *M. sancta*. Ants were collected in southwestern France, near Narbonne, and then reared in the laboratory at 25°C with 12 h light/12 h dark. Colonies were housed in several glass test tubes placed in 27 × 27-cm plastic boxes whose sides were coated with Fluon to prevent ants from escaping. Ants were provided with water in the form of moist cotton, fed *ad libitum* with a mixture of seeds and twice a week with bits of crickets.

**Experiments.** The experimental arena is a circular structure (of two possible diameters,  $\varnothing = 25$  or 50 cm) below which the nest box is located. The ants can access the arena by climbing on a wood rod placed in a hole at the center of the arena and randomly walk to the periphery. The experimental setup was designed to reduce the problem to a one-dimensional system with periodic boundary conditions: because the ants exhibit strong thigmotaxis (a tendency to follow the inner walls), their paths can be considered to be confined to one dimension. Corpses are initially homogeneously distributed along the periphery, close to the inner wall (Fig. 1a). Two different initial numbers of corpses are used in both arena sizes: 100/200 and 200/400 for the small and large arena, corresponding to 127 and 255 corpses  $m^{-1}$ , respectively. The average size of the corpses is 3 mm, the initial mean distance between them being 4.9 and 0.9 mm for the small and high density, respectively. The duration of the experiments was set to 24 hr with the small arena and 48 hr with the large arena. Fifteen replications were performed for each density with the small arena and 25 replications with the large arena. Another set of 10 experiments was performed with the large arena and a small initial number of corpses corresponding to 13 corpses  $m^{-1}$  to test the existence of a critical density of corpses. The duration of these experiments was set to 24 hr. The floor of the arena was washed with diluted alcohol and hexane before each experiment.

**Recording and Data Analysis.** The experiments were videotaped by means of a Sony (Tokyo) DCR-VX1000E high-definition camera allowing the regular sampling of the aggregation process. Two seconds of images were recorded every 10 min. A video analysis was then performed with a specially designed software that calculated the position and the size of the piles at each time interval. Two neighboring corpses are considered to belong to the same pile when the distance between them is less than 1.5

Abbreviation: LALI, local activation–long range inhibition.

<sup>†</sup>To whom reprint requests should be addressed. E-mail: theraula@cict.fr.

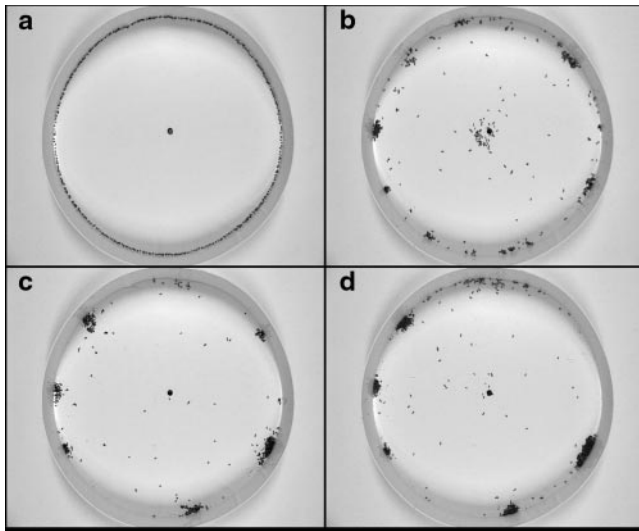


**Fig. 1.** An example of aggregation dynamics observed for an arena of  $\varnothing = 50$  cm and with  $n = 400$  corpses. (a) At  $t = 0$ ; (b) after 6 h; (c) after 12 h; (d) after 45 h.

mm (half the average size of a corpse). A pile is defined as a cluster of at least five corpses. The individual behavior of ants was studied with a separate set of experiments. The spontaneous probabilities for an ant to drop a corpse or to make a U-turn during walking were estimated by calculating the regression line of the survivorship curves of these events. The probabilities of picking up and dropping a corpse as a function of the size of the pile encountered by an ant were estimated by a series of experiments during which piles with predefined sizes were created. The size of the piles was kept constant during these experiments. Ants' trajectories were digitized by using a GrafBar GP-7 sonic digitizer (Science Accessories, Southport, CT). We put a glass plate over the active area of the digitizer and placed behind it a 13-inch video monitor. As an ant moved on the screen, it was followed with the digitizer cursor, and its path was input into a microcomputer as a series of  $X$ - $Y$  Cartesian coordinates at a rate of five points per second. Because the speed at which the ants were moving on the screen was relatively slow, ants could be followed with the videotapes played at normal speed. Digitized trajectories were used to compute the running velocity of ants, defined as the ratio of total trajectory length over the time the animal spent moving during the trajectory.

## Results

**Clustering Behavior: Collective and Individual Levels.** After having reached the arena, workers pick up corpses and drop them to form piles. After a few hours, several clusters are formed. Over time, some clusters grow and others disappear, leading to an apparent steady state with a stable number of clusters over the duration of the experiment (Fig. 1 *b–d*). The sigmoidal growth of surviving clusters, an illustration of which is given in Fig. 2, suggests that cluster formation is autocatalytic. The number of clusters initially grows to reach a maximum after about 3 hr and then decreases and stabilizes.

The above results suggest a LALI mechanism: because the addition of corpses to a cluster is more likely as the cluster increases in size, cluster growth is locally self-enhancing and is inhibited by the depletion of corpses in the cluster's neighborhood. This type of LALI model, coined "activator-substrate" (9), has been suggested in the formation of certain seashell patterns (4). To confirm this conjecture, the underlying microscopic rules have to be identified. Observation of the ants' behavior shows

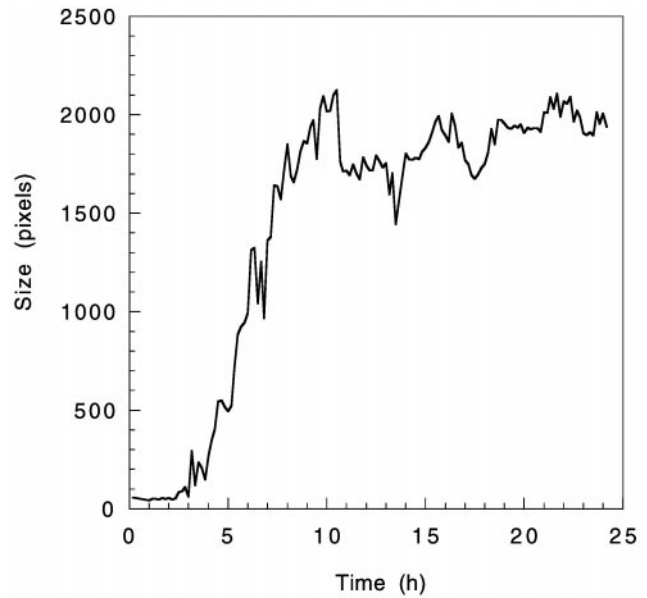


**Fig. 2.** An example of growth of a surviving cluster of corpses for an arena of  $\varnothing = 25$  cm and with  $n = 100$  corpses.

that workers pick up or drop corpses with a probability that depends on the local density ( $c$ ) of corpses. Picking up and dropping probabilities and their functional form have been estimated from experimental data (Fig. 3 *a* and *b*). Unladen ants pick up corpses with a probability that decreases with cluster size, whereas corpse-carrying ants drop corpses with a probability that increases with cluster size. The latter ants are also characterized by a spontaneous dropping probability that has been estimated from experimental data (Fig. 3 *c*). Trajectory measurements show that the ants move randomly along the arena's periphery (one-dimensional random walk) and allow the identification of two additional microscopic characteristics: individual velocity and mean free path. The mean velocity of ants is  $v = 1.6 \pm 0.7$  cm·s<sup>-1</sup> ( $n = 25$ ), and for such parameter range, random walk can be shown to be only little influenced by the velocity distribution. Further discussion will therefore assume a constant velocity of walking at the average velocity value. Ants are also characterized by a constant probability per unit of time of making a U-turn during their walk (0.10 s<sup>-1</sup>), and the corresponding mean free path ( $l = 15.8$  cm) is significantly smaller than the size of the arena's periphery (78.5 and 157.1 cm for the arena sizes used in the experiments).

**Model Description.** These estimates of microscopic behavioral parameters and the response functions have been used to build a macroscopic mathematical model that falls within the activator-substrate class of LALI models, which thus confirmed our previous assumptions. The model involves two variables: the density of corpse-carrying ants  $a(x, t)$  and the density of corpses  $c(x, t)$ , where  $x$  and  $t$  stand for space and time, respectively.  $\rho$  is the density of noncarrying ants. At any given time, their proportion in experiments is large ( $\rho/(a + \rho) = 0.94 \pm 0.07$ , estimated over 135 observations; mean density  $\bar{\rho} \pm \text{SD} = 20.0 \pm 7.0$  m<sup>-1</sup>). Because of the diffusion process resulting from the random walk of noncarrying ants,  $\rho$  is assumed to remain uniform and constant over time in the model. Ants' behavior can then be approximated by the following reaction–diffusion equations:

$$\frac{\partial c}{\partial t} = \Omega(c, a) \quad [1]$$

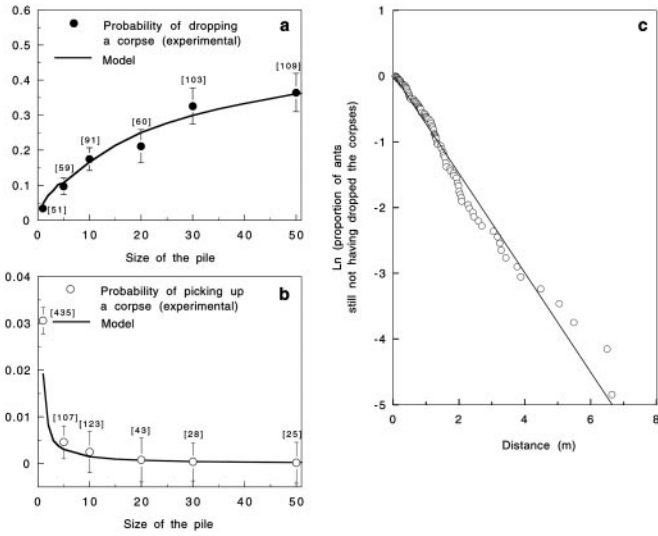


**Fig. 3.** Density-dependent probabilities of dropping (a) and picking (b) a corpse, as estimated from experiments and theoretical fittings of the dropping and picking rates (continuous line). The total number of ants dropping and picking up corpses for each size of pile is indicated in brackets. The theoretical fitting is obtained by using the Eqs. 1–3. A pile of corpses is introduced in the theoretical setup to reproduce the experimental procedure. The fraction of corpse-carrying ants crossing the pile and dropping their load gives the rate of dropping for this pile. This fraction is computed for different pile sizes. The comparison between this theoretical fraction and the corresponding experimental one provides an estimate of the parameters of the dropping function  $\alpha_1$  and  $\alpha_2$ . The same procedure is used to adjust the picking rate ( $\alpha_3$  and  $\alpha_4$ ), for which the fraction of laden ants leaving the cluster was measured. Adjusted values  $\alpha_1 = 31.75 \text{ m}^{-1}$ ,  $\alpha_2 = 1,000 \text{ m}^{-1}$ ,  $\alpha_3 = 3.125 \text{ m}^{-1}$  and  $\alpha_4 = 50 \text{ m}^{-1}$  were obtained with  $k_d = 0.75 \text{ m}^{-1}$ ,  $\rho = 40/\pi\phi \text{ m}^{-1}$ ,  $\Delta = 1 \text{ cm}$ ,  $v = 1.6 \cdot 10^{-2} \text{ m}\cdot\text{s}^{-1}$ ,  $l = 15.8 \cdot 10^{-2} \text{ m}$  and  $D = v l/2 = 1.3 \cdot 10^{-3} \text{ m}^2\cdot\text{s}^{-1}$  (see Eqs. 2 and 3). (c) The natural log of the proportion of ants ( $n = 127$ ) still carrying a corpse as a function of the distance covered since they had picked it up. The relationship is best described by the natural log of the proportion of ants that did not yet dropped the corpse they carry =  $-k_d x$  with  $k_d = 0.75 \text{ m}^{-1}$  ( $r^2 = 0.975$ ;  $x$  is the distance in m).

$$\frac{\partial a}{\partial t} = -\Omega(c, a) + D \frac{\partial^2 a}{\partial x^2}, \quad [2]$$

where  $\Omega(c, a)$  is the sum of three terms:

$$\Omega(c, a) = v \left[ \frac{k_d a}{I} + \frac{\alpha_1 a \phi_c}{\alpha_2 + \phi_c} - \frac{\alpha_3 \rho c}{\alpha_4 + \phi_c} \right]. \quad [3]$$

In Eq. 3,  $v$  is the linear velocity of the ants, part I represents spontaneous dropping (with  $k_d$  the spontaneous dropping rate per laden ants), and parts II and III represent density-dependent dropping and picking, respectively. I and II are proportional to the density of corpse-carrying ants ( $a$ ), and III is proportional to noncarrying ants ( $\rho$ ).  $\alpha_1$ ,  $\alpha_2$ ,  $\alpha_3$ , and  $\alpha_4$  are empirical constants.  $\phi_c$  is a nonlocal term that introduces a short-range interaction between workers and corpses:

$$\phi_c = \frac{1}{2\Delta} \int_{x-\Delta}^{x+\Delta} c(z) dz,$$

where  $\Delta$  is a small radius of perception within which workers can detect corpses (dedicated experimental measurements lead to a characteristic radius of  $0.5 \text{ cm} < \Delta < 1.0 \text{ cm}$ ). The dropping rate

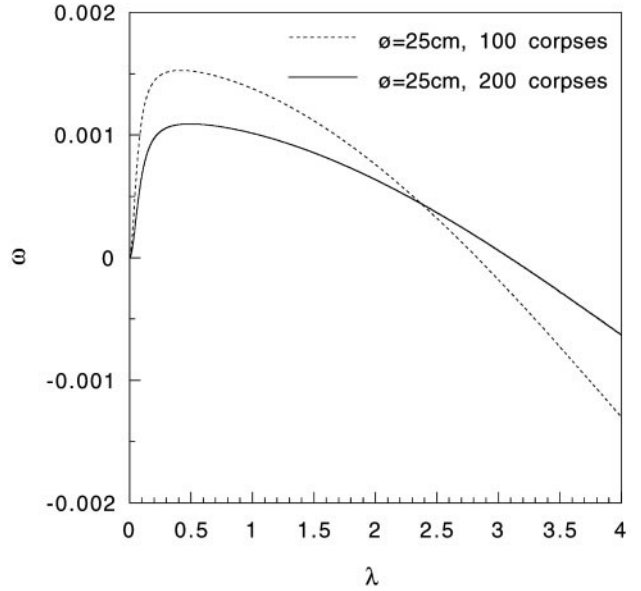


**Fig. 4.** Stability analysis of the steady states. Solution of the characteristic equation as a function of the wave number  $\lambda$  for the experimental conditions  $\phi = 25 \text{ cm}$ , 100 corpses and 200 corpses. The parameter values are those of Fig. 3 legend.

per laden ants (II) increases with  $\phi_c$  and reaches the asymptotic value  $v\alpha_1$ . The picking rate per noncarrying ants (III) results from the presence of noncarrying ants picking available corpses. It decreases when  $\phi_c$  increases. Therefore, according to III, cluster size acts as a negative feedback on the picking rate, because  $\phi_c$  is a local indicator of cluster size. As a result of II and III, clusters form, and their growth inhibits the further growth of other clusters. A standard stability analysis, where a perturbation around the unique homogeneous steady state ( $c_s, a_s$ ) is introduced ( $c = c_s + \delta c_0 e^{\omega t + i\lambda x}$ ;  $a = a_s + \delta a_0 e^{\omega t + i\lambda x}$ ), leads to the characteristic equation:

$$\omega^2 + (-\Gamma + \Phi + D\lambda^2)\omega - \Gamma D\lambda^2 = 0, \quad [4]$$

where

$$\Gamma = \frac{\sin(\lambda\Delta)}{\lambda\Delta} \left( \frac{\alpha_2 \alpha_1 a_s}{(\alpha_2 + c_s)^2} + \frac{\alpha_3 \rho c_s}{(\alpha_4 + c_s)^2} \right) - \frac{\alpha_3 \rho}{(\alpha_4 + c_s)}$$

$$\Phi = k_d + \frac{\alpha_1 c_s}{(\alpha_2 + c_s)}.$$

Solving Eq. 4 for  $\omega$  yields the rate of growth  $\omega(\lambda)$  of the perturbation for a given wave number  $\lambda$ . Here  $\omega(\lambda)$  exhibits a finite range of unstable modes that includes the marginally stable mode  $\omega(0) = 0$  (Fig. 4). This is a well-known property of systems involving a conservation law. Furthermore, as is usual with such models, the most unstable wave number, that is the one for which  $\omega(\lambda)$  is maximum, is proportional to corpse density. In other words the analysis predicts (i) that in the vicinity of the homogeneous state, doubling corpse density should lead to twice as many piles; this situation may change over time as the system relaxes away from the homogeneous state as other unstable wave numbers may become amplified; (ii) that doubling the arena's diameter while keeping the density constant should lead to twice as many piles; (iii) that a critical density of corpses exists ( $c_c = 46 \text{ corpses m}^{-1}$ ) below which no aggregation occurs.

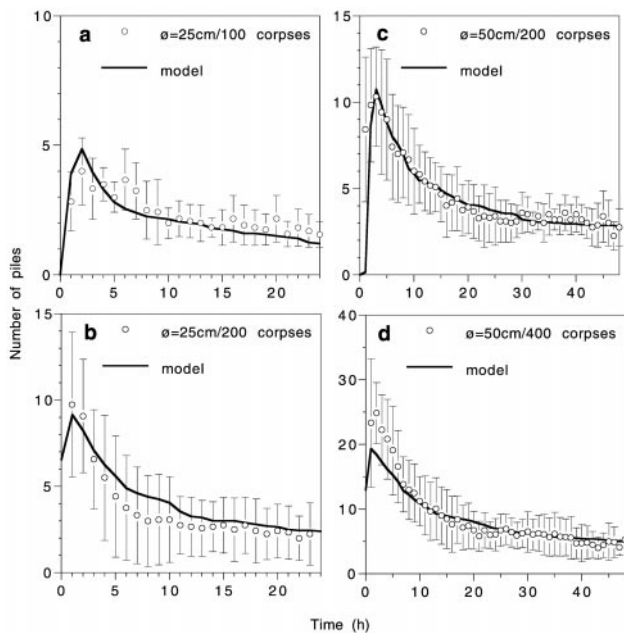


**Fig. 5.** Evolution as a function of time of the mean number of clusters (a cluster contains at least five corpses) obtained from 20 integrations of the model equations (full lines) and of the number of clusters obtained experimentally (average and SD are given for six experiments per condition) in four experimental conditions. (a)  $\varnothing = 25$  cm, 100 corpses; (b)  $\varnothing = 25$  cm, 200 corpses; (c)  $\varnothing = 50$  cm, 200 corpses; (d)  $\varnothing = 50$  cm, 400 corpses. The initial conditions (spatial distribution of corpses) are randomly set around the value ( $c_3$ ). The parameter values used in the model are those of Fig. 3 legend.

**Comparison of the Model's Predictions with Experimental Results.** As shown in Fig. 5, the dynamics of the average number of piles with time and the time at which the maximum number of piles is reached given by the model are in close agreement with the experiments in the four conditions studied. In particular, predictions of the stability analysis are confirmed in the initial phase (up to maximum pile number): (i) doubling the density leads to a doubling of the number of piles; (ii) doubling the arena's diameter, whereas keeping the same density also leads to twice as many piles; (iii) in experiments performed with an initial density of corpses ( $13 \text{ corpses m}^{-2}$ ) below, no stable clusters were observed. In situations where several piles coexist after 24 or 48 hr (far from the homogenous state), although no strict regularity may be noticed, a critical distance exists between two consecutive piles below which only one of them can "survive" in the long term as shown in Fig. 6. After 24 hr, with the small arena and whatever the initial density of corpses, the presence of two consecutive piles within 20 cm of each other is very unlikely. In any case, the distance between piles is never less than 10 cm. The most frequent distribution, with piles located on opposite sides of the arena, is observed in 50% of the cases. The corresponding theoretical distribution is not significantly different from the experimental one, and both distributions differ significantly from a random distribution (Fig. 6).

## Discussion

The observation of cemetery formation in ant colonies suggests a LALI mechanism based on individual worker behavior. It is a peculiar example of such mechanisms in that it involves animal

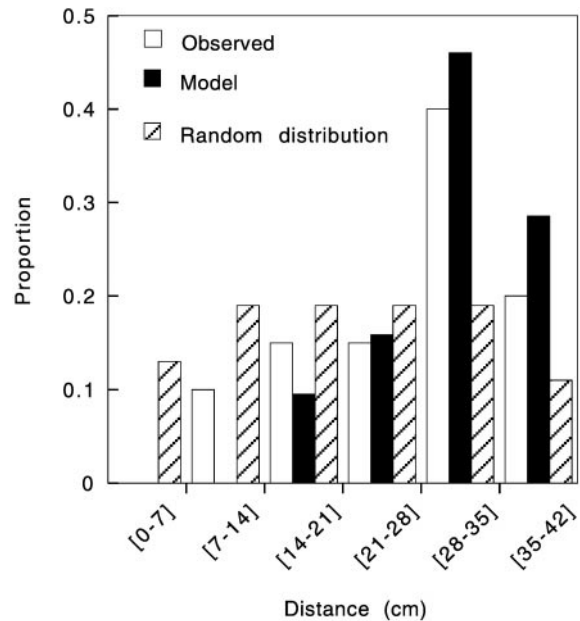


**Fig. 6.** Comparison between theoretical ( $n = 47$ ) and experimental ( $n = 21$ ) distributions of distances between two consecutive clusters in the conditions  $\varnothing = 25$  cm, 100 corpses and  $\varnothing = 25$  cm, 200 corpses in the case where only two clusters remain after 24 hr. There is no statistical difference between experimental and theoretical distributions (Kolmogorov–Smirnov test performed on distances,  $P > 0.334$ ,  $Z = 0.945$ ) and both distributions are statistically different of a random distribution,  $n = 5 \cdot 10^3$  (Kolmogorov–Smirnov test performed on distances,  $P < 0.05$ ,  $Z = 1.543$  and  $P < 0.001$ ,  $Z = 3.636$  respectively). The random distribution is generated as follows: the positions of the two clusters are independent of each other, except that they cannot overlap. The probability that the distance is less than the length of the pile ( $L = 4$  cm) is 0 and the probability  $P(l)$  to have a distance  $l$  greater than  $L$  and smaller than  $0.5\pi\varnothing$  is  $P(l) = 1/[0.5\pi\varnothing - L]$ .

behavior and not physical and chemical morphogens. All of the behavioral parameters of the corresponding model were quantified in dedicated experiments. When loaded with the experimental parameter values, the model not only leads to the formation of patterns that reproduce the properties of cemetery formation, but also predicts how the pattern is affected by such experimental characteristics as corpse density and arena size. Experiments aimed at testing the model's predictions show that the predictions are indeed satisfied. This is a strong indication that the formation of cemeteries in ants is an example of LALI morphogenesis, which makes it one of the first convincing documented biological examples and certainly the first involving higher organisms. Our work should encourage researchers to look for such mechanisms in other collective behavioral patterns such as network formation (33, 34), nest construction (29–31, 39), or herd patterns (40, 41), where it could be easier to identify the underlying activation and inhibition mechanisms than in other systems.

We thank S. Foucaud and F. Villeneuve-Séguier for technical assistance and discussions and P. Borckmans, G. Dewel, and R. Lefever for helpful comments on an earlier draft. This work was supported by the Santa Fe Institute and by grants from the Conseil Régional Midi-Pyrénées and the Groupement d'Intérêt Scientifique "Sciences de la Cognition."

- Ball, P. (1998) *The Self-Made Tapestry* (Oxford, New York).
- Murray, J. D. (1990) *Mathematical Biology* (Springer, Berlin).
- Ermentrout, B., Campbell, J. & Oster, G. F. (1986) *Veliger* **28**, 369–388.
- Meinhardt, H. (1995) *The Algorithmic Beauty of Sea Shells* (Springer, Berlin).
- Swindale, N. V. (1980) *Proc. R. Soc. London Ser. B* **208**, 243–264.

- Bascompte, J. & Solé, R. V. (1998) *Trends Ecol. Evol.* **13**, 173–174.
- Turing, A. (1952) *Philos. Trans. R. Soc. London B* **237**, 37–72.
- Glansdorff, P. & Prigogine, I. (1971) *Thermodynamics of Structure, Stability, and Fluctuations* (Wiley, London).
- Gierer, A. & Meinhardt, H. (1972) *Kybernetik* **12**, 30–39.

10. Segel, L. A. & Jackson, J. L. (1972) *J. Theor. Biol.* **37**, 545–549.
11. Meinhardt, H. (1982) *Models of Biological Pattern Formation* (Academic, London).
12. Oster, G. F. (1988) *Math. Biosci.* **90**, 265–286.
13. Manneville, P. (1990) *Dissipative Structures and Weak Turbulence* (Academic, San Diego).
14. Castets, V., Dulos, E., Boissonade, J. & De Kepper, P. (1990) *Phys. Rev. Lett.* **64**, 2953–2957.
15. Lefever, R. & Lejeune, O. (1997) *Bull. Math. Biol.* **59**, 263–294.
16. Kareiva, P. & Odell, G. (1987) *Am. Nat.* **130**, 233–270.
17. Kareiva, P. (1984) in *Mathematical Ecology*, Levin, S. & Hallam, T., eds. (Springer, Berlin), Springer Lectures Notes in Biomathematics, Vol. 54, 368–389.
18. Kareiva, P. (1987) *Nature (London)* **326**, 388–390.
19. Freeman, M. (2000) *Nature (London)* **408**, 313–319.
20. Meinhardt, H. (2001) *Int. J. Dev. Biol.* **45**, 177–188.
21. Buikema, W. J. & Haselkorn, R. (2001) *Proc. Natl. Acad. Sci. USA* **98**, 2729–2734.
22. Yoon, H. S. & Golden, J. W. (1998) *Science* **282**, 935–938.
23. Keller, E. F. & Segel, L. A. (1971) *J. Theor. Biol.* **30**, 235–248.
24. Nijhout, H. F. (1990) *Proc. R. Soc. London Ser. B* **239**, 81–113.
25. Kondo, A. & Asai, R. (1995) *Nature (London)* **376**, 765–768.
26. Painter, K. J., Maini, P. K. & Othmer, H. G. (1999) *Proc. Natl. Acad. Sci. USA* **96**, 5549–5554.
27. Keller, E. F. & Segel, L. A. (1970) *J. Theor. Biol.* **26**, 399–415.
28. Sawai, S., Maeda, Y. & Sawada, Y. (2000) *Phys. Rev. Lett.* **85**, 2212–2215.
29. Deneubourg, J. L. (1977) *Ins. Soc.* **2**, 117–130.
30. Bonabeau, E., Theraulaz, G., Deneubourg, J. L., Franks, N., Rafelsberger, O., Joly, J. L. & Blanco, S. (1998) *Philos. Trans. R. Soc. Lond. B* **353**, 1561–1576.
31. Camazine, S., Sneyd, J., Jenkins, M. J. & Murray, J. D. (1990) *J. Theor. Biol.* **147**, 553–571.
32. Cole, B. J. & Cheshire, D. (1996) *Am. Nat.* **148**, 1–15.
33. Edelstein-Keshet, L. (1994) *J. Math. Biol.* **32**, 303–328.
34. Edelstein-Keshet, L., Watmough, J. & Ermentrout, G. B. (1995) *Behav. Ecol. Soc.* **36**, 119–133.
35. Haskins, C. P. & Haskins, E. F. (1974) *Psyche* **81**, 258–267.
36. Howard, D. F. & Tschinkel, W. R. (1976) *Behaviour* **56**, 157–180.
37. Ataya, H. & Lenoir, A. (1984) *Ins. Soc.* **31**, 20–33.
38. Gordon, D. (1983) *J. Chem. Ecol.* **9**, 105–111.
39. Skarka, V., Deneubourg, J. L. & Belic, M. R. (1990) *J. Theor. Biol.* **147**, 1–16.
40. Gueron, S. & Levin, S. A. (1993) *J. Theor. Biol.* **165**, 541–552.
41. Parrish, J. K. & Edelstein-Keshet, L. (1999) *Science* **284**, 99–101.